Microscopy and Microanalysis, **31** (7), 2025, 1527–1530
https://doi.org/10.1093/mam/ozaf048.785

Microscopy AND Microanalysis

Proceedings

Fever State Simulation to Study the Behavior of Novel Ti-Mn Alloys for Medical Devices

Sofia Sakr-Nassef[1], Cristina Jiménez-Marcos[1], Julia Claudia Mirza-Rosca[1,2,*], and Ionelia Voiculescu[3]

[1]*Department of Mechanical Engineering, University of Las Palmas de Gran Canaria, Las Palmas de Gran Canaria, Spain.*
[2]*Materials Engineering and Welding Department, Transilvania University of Brasov, Brasov, Romania*
[3]*Faculty of Industrial Engineering and Robotics, Politehnica University of Bucharest, Bucharest, Romania*

*Corresponding author: julia.mirza@ulpgc.es

The development of new biocompatible materials is necessary to improve the durability and effectiveness of medical implants. Titanium alloys have received much attention due to their corrosion resistance [1], proven biocompatibility [2], and ideal strength-to-weight ratio. Consequently, Ti alloys are used in the chemical, aerospace, automotive, and even biomedical industries [3].

Titanium has excellent corrosion resistance due to its low density and innate capacity to form a protective oxide layer, which lowers the likelihood of adverse biological interactions. Adding elements to titanium, such as manganese, can change the electrochemical behavior of titanium and improve its mechanical properties, which would be very beneficial for biomedical applications [4].

The research focuses on analyzing the structure, corrosion at elevated temperatures, and hardness of two Ti-Mn alloys for medical implants. The aim is to determine the effect of composition on the alloys' mechanical strength and chemical stability, aiming to create biometrically safe and efficient materials. Higher temperatures can affect implant durability.

The materials used in this research are called Ti3Mn and Ti4Mn, whose composition is presented in Table 1. For the microstructural, electrochemical, and nanoindentation tests, the alloy ingots were cut into three pieces (S180, S200, and S250 samples) using a Buehler IsoMet 4000 precision saw. The specimens were then embedded in epoxy resin using a 4:1 catalyst mixture; after 24 hours, the specimens were demoulded. The samples were then ground and polished using the Struers TegraPol-11 polisher with progressive silicon carbide papers from 400 to 2500 grit and finally polished to a final mirror finish using 0.1-micron alpha alumina suspension polishing cloths (see Fig. 1).

The embedded samples were subjected to electrochemical testing, microhardness testing, and microstructural examination. Following chemical etching of the samples using Kroll reagent (100 ml water, 1-3 ml hydrofluoric acid, and 2-6 ml nitric acid), structural characterization was performed using the ZEISS Axio Vert.A1 MAT microscope. To determine the corrosion potential and rate as well as to perform electrochemical impedance spectroscopy (EIS), continuous and alternating current electrochemical experiments were conducted using the BioLogic Essential SP-150 potentiostat and a simulated bodily fluid (SBF) called Lactato Ringer at 40°C. Ten measurements are taken applying 5, 25 and 50 gf in the Vickers hardness test using the Affri DM8 B hardness tester.

The surface structures of the samples after chemical etching using the metallography technique are shown in Fig. 2. Equiaxial grains with sharp outlines, typical of the α-phase (HCP) of titanium, can be distinguished with slightly darkened grain boundaries, indicating the presence of small amounts of β at the grain boundaries.

Following ten hardness tests with three distinct loads for every sample, Fig. 3 shows that Ti4Mn exhibits a higher hardness for every indentation than Ti3Mn at the 5 gf load, along with a bigger standard deviation. The specimens' standard deviation drops while Ti3Mn's hardness values significantly increase at 25 and 50 gf loads.

In the case of the electrochemical tests shown in Fig. 4, the corrosion potential of both samples has tended to passivate, with a higher stability for Ti4Mn, but with a more positive potential value for Ti3Mn. In turn, the corrosion rate obtained for the two samples was similar, being higher for Ti3Mn with $1.29{\cdot}10^{-3}$ mpy and lower for Ti4Mn with $2.52{\cdot}10^{-3}$ mpy. Applying EIS for the positive potentials of 0.2, 0.4 and 0.6 V vs. reference electrode, a similar capacitive behavior with a slight decrease of the impedance values as more positive potentials are applied is observed in the Nyquist plots of both samples. In turn, in the Bode impedance and Bode phase diagrams of these samples, the maximum impedance and phase angles values remain practically constant for both samples, higher for Ti3Mn (about $1.85{\cdot}10^{4}$ Ohm·cm^2 and 72°) than for Ti4Mn (about $1.3{\cdot}10^{4}$ Ohm-cm^2 and 71°). The equivalent circuit best fitted to both samples is R_1 $(C_2R_2)(Q_2R_2)$, where R_1 is the dissolution resistance, C_2 and R_2 are the capacitor and the resistance of the passive porous layer of the sample surface, and Q_3 and R_3 are the phase constant element and the resistance of the passive compact layer.

Research on the Ti-Mn Alloys gives more information regarding the mechanical behavior of his alloys. The microstructure shows well rounded equiaxial alpha phase grains which improve the mechanical performance. In the hardness tests, it was observed that Ti4Mn shows higher hardness at lower loads, but with extreme variation, while at higher loads, Ti3Mn shows greater stability. The electrochemical tests are concentrated on the positive corrosion potential of Ti3Mn, whereas, for Ti4Mn, greater stability is observed. The impedance spectra ascertained the best surface protection for Ti3Mn at lower frequencies. These results provide valuable insight into how Ti-Mn alloys function in biomedical applications while stimulating further simulated and experimental work in vivo dynamic conditions.

Table 1. Composition (in wt%) of the alloys under study.

	Composition (in wt%)				
Sample	Ti	Mn	Al	Fe	V
Ti3Mn	96.2	3.0	0.6	-	0.2
Ti4Mn	94.4	4.0	0.6	1.0	-

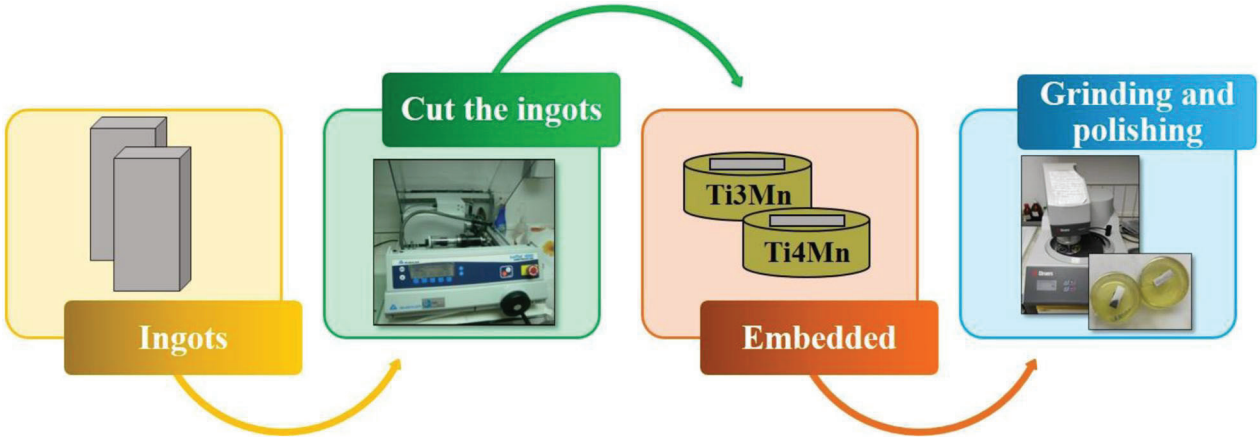

Fig. 1. Preparation of the samples for study.

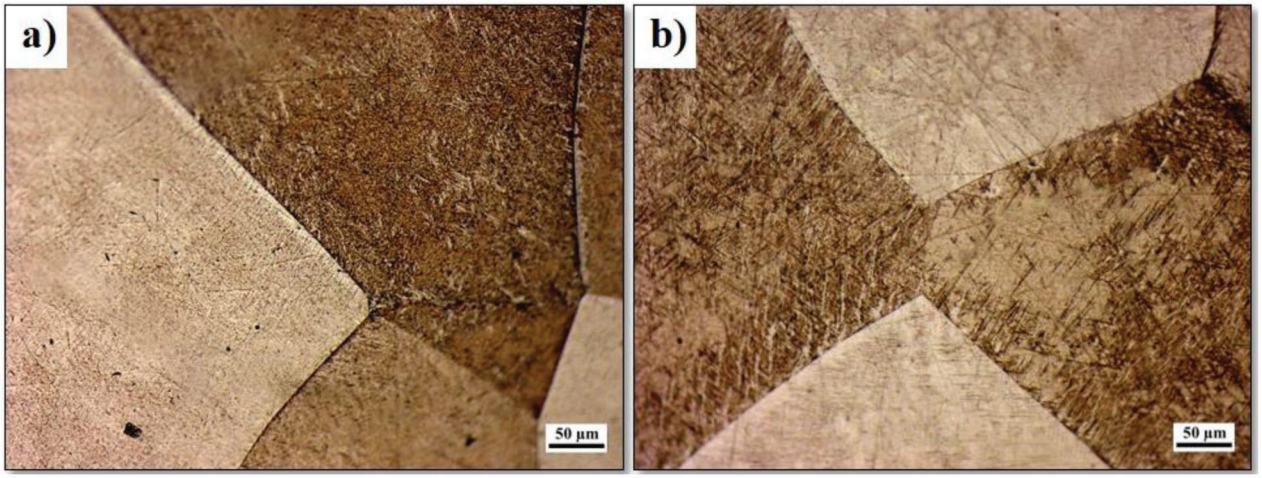

Fig. 2. Microstructure of Ti3Mn (a)) and Ti4Mn (b)) samples at x10 magnification.

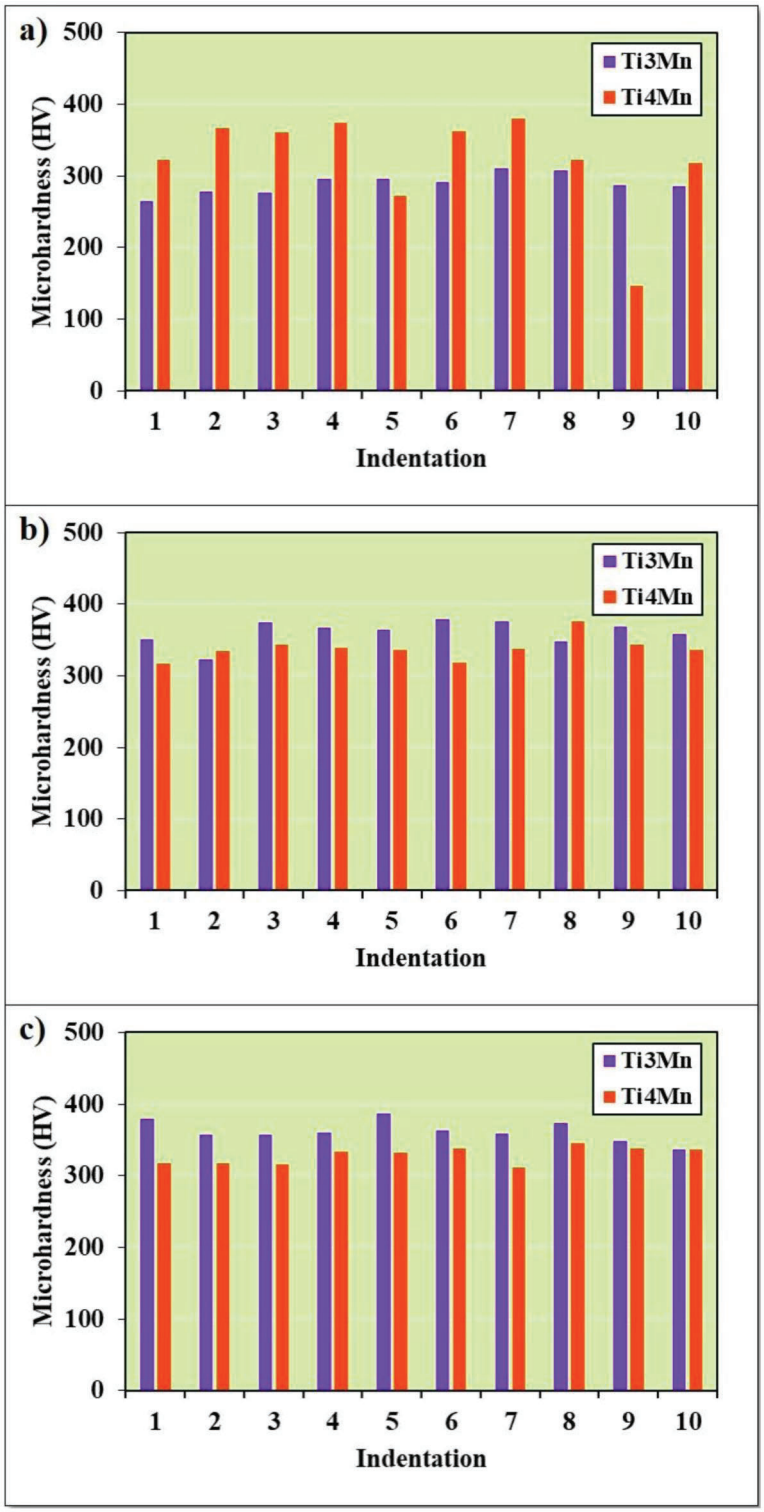

Fig. 3. Microhardnes values for each indentation of each sample applying loads of 5 (a)), 25 (b)) and 50 (c)) gf.

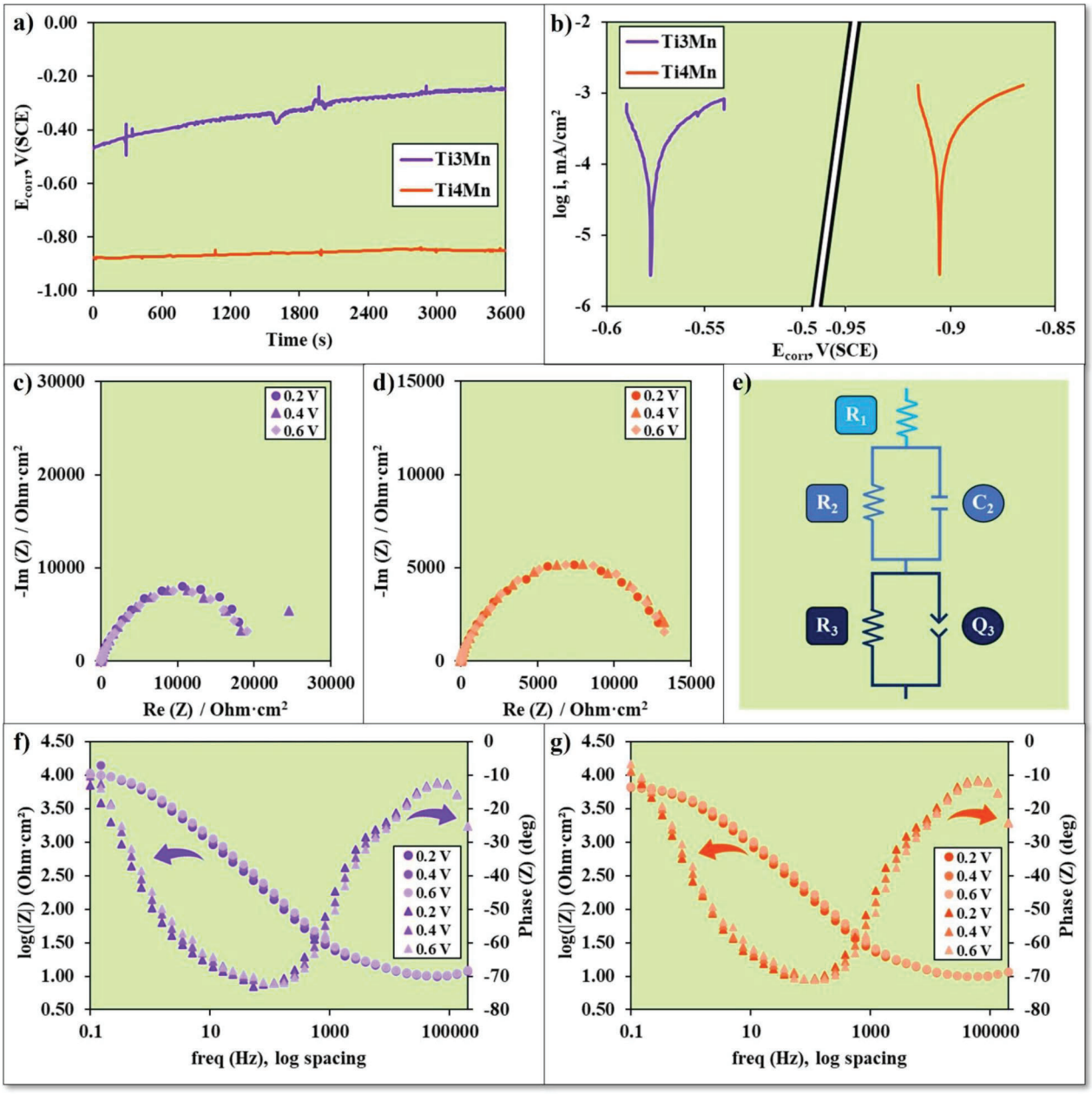

Fig. 4. Corrosion potential (a)), corrosion rate (b)), Nyquist diagram for Ti3Mn (c)) and Ti4Mn (d)) samples, equivalent electrical circuit applied (e)), Bode impedance and phase diagram for Ti3Mn (f)) and Ti4Mn (g)) samples.

References

1. Vasilescu, E.; Drob, P.; Popa, M. V.; Anghel, M.; Santana Lopez, A.; Mirza-Rosca, I. Characterisation of anodic oxide films formed on titanium and two ternary titanium alloys in hydrochloric acid solutions. *Werkstoffe und Korrosion* 2000, **51**, 413–417, doi:10.1002/1521-4176(200006)51:6<413::AID-MACO413>3.0.CO;2-3.
2. Lopez, A.S.; Mirza-Rosca, J.; Vasilescu, E.; Drob, P.; Raducanu, D.; Angelescu, L. Technical and functional properties of some biocompatible thin films. *Mater. Chem. Phys*. 2004, **86**, 38–43, doi:10.1016/j.matchemphys.2004.01.016.
3. Jimenez-Marcos, C.; Mirza-Rosca, J.C.; Baltatu, M.S.; Vizureanu, P. Experimental Research on New Developed Titanium Alloys for Biomedical Applications. *Bioengineering* 2022, **9**, 686, doi:10.3390/bioengineering9110686.
4. Ionithã, D.; Santana Lopez, A.; Mirza-Rosca, J.; Vasilescu, E.; Popa, M.V.; Drob, P.; Vasilescu, C. Electrochemical impedance spectroscopy technique in prediction of the implant titanium alloys behaviour. *Eur. Cells Mater*. 2003, 5.